# Wigner-Function Based Simulation of Classic and Ballistic Transport in Scaled DG-MOSFETs Using the Monte Carlo Method

A. Gehring and H. Kosina

Institute for Microelectronics, TU Vienna, Gußhausstraße 27–29, A-1040 Wien, Austria
gehring@iue.tuwien.ac.at

Double-gate (DG) MOS transistor structures have been proposed to boost the performance of scaled-down logic devices and to overcome some of the most severe problems encountered in bulk MOS field-effect transistors [1]. However, with channel lengths below 25 nm, the question of the importance of quantum effects in the lateral direction, such as source-to-drain tunneling, arises. Frequently, ballistic transport is assumed which allows the device to be simulated using pure quantum-mechanical approaches [2–4]. However, with carrier mean free paths in the range of several nanometers, scattering-limited transport may still be dominant which can be assessed using the Monte Carlo method by accounting for quantum-correction methods [5, 6]. An approach accounting for both, quantum interference phenomena and scattering processes, is based on the Wigner equation augmented by the Boltzmann collision operator,

$$\left(\frac{\partial}{\partial t} + \mathbf{v}\cdot\nabla_r + \frac{\mathrm{q}\mathbf{E}}{\hbar}\cdot\nabla_k\right) f_w = \int V_w(\mathbf{r},\mathbf{k}-\mathbf{k}') f_w(\mathbf{k}',\mathbf{r},t)\,\mathrm{d}\mathbf{k}' + \left(\frac{\partial f_w}{\partial t}\right)_{\mathrm{coll}}$$

with the Wigner potential defined by

$$V_w(\mathbf{r},\mathbf{k}) = \frac{1}{\imath\hbar\,(2\pi)^3}\int \left(V(\mathbf{r}+\tfrac{\mathbf{s}}{2}) - V(\mathbf{r}-\tfrac{\mathbf{s}}{2}) + \mathrm{q}\mathbf{s}\cdot\mathbf{E}\right) e^{-\imath\mathbf{k}\cdot\mathbf{s}}\,\mathrm{d}\mathbf{s}$$

This equation can be solved using the Monte Carlo method [7, 8]. We report on the enhancement of the Wigner Monte Carlo simulator described in [8] for the simulation of silicon-based devices. The algorithm for annihilation of numerical particles now takes into account the multi-valley band structure of silicon. As test devices we use double-gate MOSFETs with gate lengths of 60 nm, 25 nm, and 10 nm. For simplicity, metal gates with midgap work function have been assumed, and a silicon dioxide thickness of 0.75 nm without wave function penetration was used. A source/drain doping of $5\times10^{19}\,\mathrm{cm}^{-3}$ with abrupt doping profile and a channel doping of $1\times10^{15}\,\mathrm{cm}^{-3}$ was chosen, as shown for the 25 nm device in Fig. 1. Transport has been calculated non-selfconsistently in the first subband calculated by lateral quantization ($\mathrm{m_l}$=0.91 $\mathrm{m_0}$), based on a drift-diffusion simulation with Minimos-NT. Fig. 2 shows the conduction band edge and the respective subband along the channel. Fig. 3 shows the Wigner generation rate along the channel for a drain bias of 0.1 V and 0.8 V in a 60 nm gate length device. The mean electron energy is shown in Fig. 4, and the corresponding carrier concentrations of a 15 nm and 10 nm gate length device are depicted in Fig. 5 for a bias of 0.1 V and 0.8 V, respectively. The output characteristics of the 25 nm device shown in Fig. 6 indicates that at this gate length, devices are still dominated by scattering and the assumption of coherent transport overestimates the current density at least by a factor of two.

[1] J.-P. Colinge, Solid-State Electron. **48**, 897 (2004).
[2] M. Lundstrom and Z. Ren, IEEE Trans.Electron Devices **49**, 133 (2002).
[3] R. Venugopal *et al.*, J.Appl.Phys. **92**, 3730 (2002).
[4] D. Munteanu and J.-L. Autran, Solid-State Electron. **47**, 1219 (2003).
[5] F. Gámiz *et al.*, Solid-State Electron. **48**, 937 (2004).
[6] G. A. Khatawala, B. Winstead, and U. Ravaioli, IEEE Trans.Electron Devices **50**, 2467 (2003).
[7] L. Shifren, C. Ringhofer, and D. K. Ferry, IEEE Trans.Electron Devices **50**, 769 (2003).
[8] H. Kosina, M. Nedjalkov, and S. Selberherr, J. Computational Electronics **2**, 147 (2002).

A full journal publication of this work will be published in the Journal of Computational Electronics

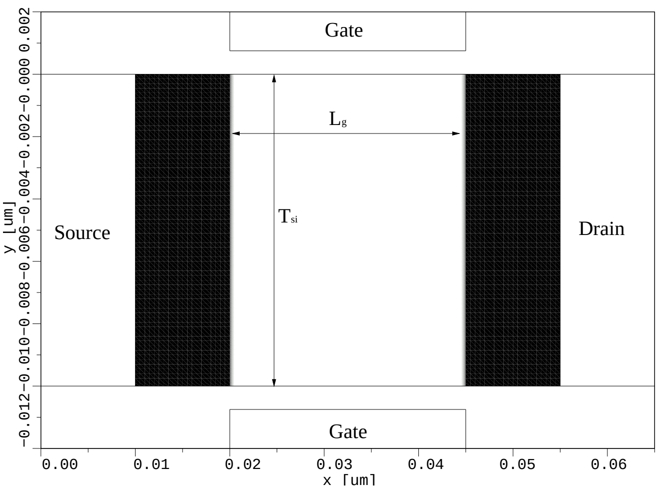


**Figure 1:** The double-gate MOS structure considered for the simulations.

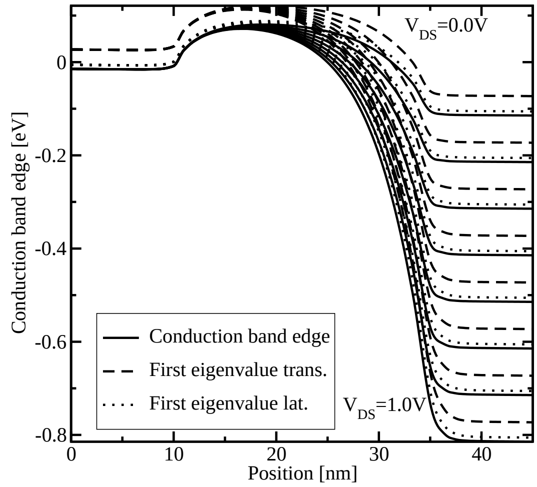


**Figure 2:** Conduction band edge and first lateral ($m_l$=0.91$m_0$) and transversal ($m_t$=0.19$m_0$) subband.

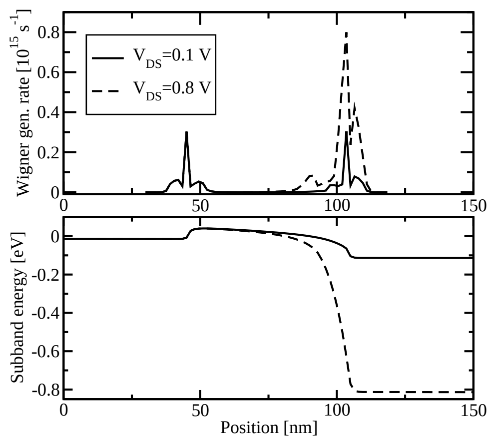


**Figure 3:** The Wigner generation rate in the 60 nm device for different drain bias.

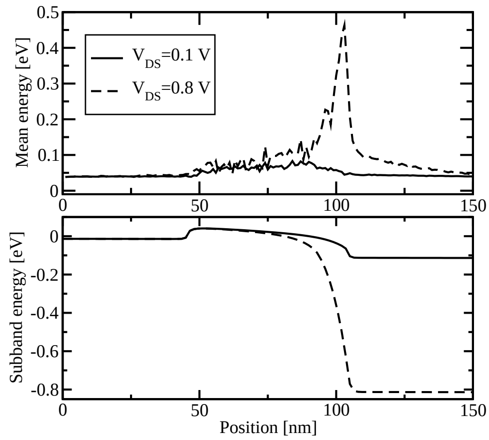


**Figure 4:** The mean particle energy in the 60 nm device for different drain bias.

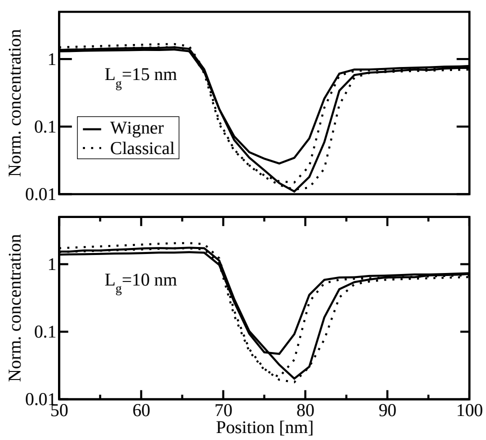


**Figure 5:** The carrier concentrations in the 15 nm (top) and 15 nm (bottom) device at different drain voltages.

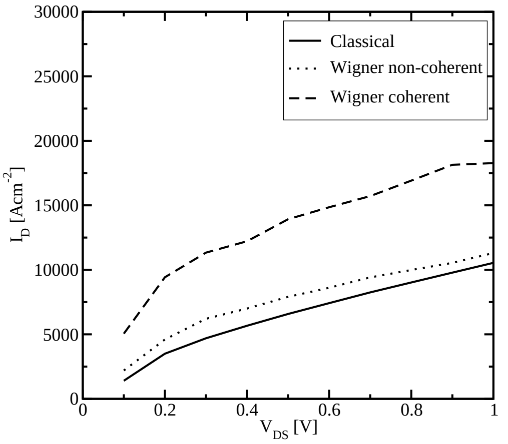


**Figure 6:** Output characteristics of the 25 nm device using classical, coherent Wigner, and non-coherent Wigner Monte Carlo.

A full journal publication of this work will be published in the Journal of Computational Electronics